Journal of Cardiovascular Computed Tomography xxx (xxxx) xxx–xxx

Contents lists available at ScienceDirect

Journal of Cardiovascular Computed Tomography

journal homepage: www.elsevier.com/locate/jcct

Artificial intelligence machine learning-based coronary CT fractional flow reserve (CT-FFR$_{ML}$): Impact of iterative and filtered back projection reconstruction techniques

Domenico Mastrodicasa[a,b,c], Moritz H. Albrecht[a,d], U. Joseph Schoepf[a,e,*], Akos Varga-Szemes[a], Brian E. Jacobs[a], Sebastian Gassenmaier[a], Domenico De Santis[f], Marwen H. Eid[a], Marly van Assen[a,g], Chris Tesche[h], Cesare Mantini[c], Carlo N. De Cecco[a,i]

[a] Division of Cardiovascular Imaging, Department of Radiology and Radiological Science, Medical University of South Carolina, Charleston, SC, USA
[b] Department of Radiology, Division of Cardiovascular Imaging, Stanford University School of Medicine, 300 Pasteur Dr, Stanford, CA, USA
[c] Department of Neuroscience and Imaging, Section of Diagnostic Imaging and Therapy - Radiology Division, SS. Annunziata Hospital, "G. d'Annunzio" University, Chieti, Italy
[d] Diagnostic and Interventional Radiology, University Hospital Frankfurt, Frankfurt, Germany
[e] Division of Cardiology, Department of Medicine, Medical University of South Carolina, Charleston, SC, USA
[f] Department of Radiological Sciences, Oncology and Pathology, University of Rome "Sapienza", Rome, Italy
[g] Center for Medical Imaging - North East Netherlands, University Medical Center Groningen, University of Groningen, Groningen, The Netherlands
[h] Department of Cardiology and Intensive Care Medicine, Heart Center Munich-Bogenhausen, Munich, Germany
[i] Department of Radiology & Imaging Sciences, Emory University, Atlanta, GA, USA

ARTICLE INFO

Keywords:
Coronary artery disease
Coronary computed tomography angiography
Iterative reconstruction
Filtered back-projection
Fractional flow reserve

ABSTRACT

Background: The influence of computed tomography (CT) reconstruction algorithms on the performance of machine-learning-based CT-derived fractional flow reserve (CT-FFR$_{ML}$) has not been investigated. CT-FFR$_{ML}$ values and processing time of two reconstruction algorithms were compared using an on-site workstation.

Methods: CT-FFR$_{ML}$ was computed on 40 coronary CT angiography (CCTA) datasets that were reconstructed with both iterative reconstruction in image space (IRIS) and filtered back-projection (FBP) algorithms. CT-FFR$_{ML}$ was computed on a per-vessel and per-segment basis as well as distal to lesions with ≥50% stenosis on CCTA. Processing times were recorded. Significant flow-limiting stenosis was defined as invasive FFR and CT-FFR$_{ML}$ values ≤ 0.80. Pearson's correlation, Wilcoxon, and McNemar statistical testing were used for data analysis.

Results: Per-vessel analysis of IRIS and FBP reconstructions demonstrated significantly different CT-FFR$_{ML}$ values ($p \leq 0.05$). Correlation of CT-FFR$_{ML}$ values between algorithms was high for the left main (r = 0.74), left anterior descending (r = 0.76), and right coronary (r = 0.70) arteries. Proximal and middle segments showed a high correlation of CT-FFR$_{ML}$ values (r = 0.73 and r = 0.67, $p \leq 0.001$, respectively), despite having significantly different averages ($p \leq 0.05$). No difference in diagnostic accuracy was observed (both 81.8%, $p = 1.000$). Of the 40 patients, 10 had invasive FFR results. Per-lesion correlation with invasive FFR values was moderate for IRIS (r = 0.53, $p = 0.117$) and FBP (r = 0.49, $p = 0.142$). Processing time was significantly shorter using IRIS (15.9 vs. 19.8 min, $p \leq 0.05$).

Conclusion: CT reconstruction algorithms influence CT-FFR$_{ML}$ analysis, potentially affecting patient management. Additionally, iterative reconstruction improves CT-FFR$_{ML}$ post-processing speed.

Abbreviations: BMI, Body mass index; CAD, Coronary artery disease; CCTA, Coronary CT angiography; CT-FFR, CT-derived fractional flow reserve; CT-FFR$_{ML}$, Machine-learning-based coronary CT-derived fractional flow reserve; CX, Left circumflex artery; FBP, Filtered back-projection; FFR, Fractional flow reserve; ICA, Invasive catheter angiography; IRIS, Iterative reconstruction in image space; LAD, Left anterior descending artery; LM, Left main artery; RCA, Right coronary artery; SD, Standard deviation

* Corresponding author. Heart & Vascular Center, Medical University of South Carolina Ashley River Tower 25 Courtenay Drive, Charleston, SC 29425-2260, USA.
E-mail address: schoepf@musc.edu (U.J. Schoepf).

https://doi.org/10.1016/j.jcct.2018.10.026
Received 20 June 2018; Received in revised form 19 October 2018; Accepted 24 October 2018
1934-5925/ Published by Elsevier Inc. on behalf of Society of Cardiovascular Computed Tomography

1. Introduction

Computational fluid dynamics (CFD) applied to coronary CT angiography (CCTA) has enabled non-invasive hemodynamic assessment of coronary artery disease (CAD).[1] CFD-based coronary CT-derived fractional flow reserve (CT-FFR) represents an established approach and has demonstrated high diagnostic accuracy for detecting lesion-specific ischemia.[2] However, powerful computational requirements limit the use of this technology to supercomputers in off-site core laboratories.[1]

With the advent of artificial intelligence, it is now possible to non-invasively derive FFR values using on-site, physician-driven workstations.[3] Several trials have reported strong diagnostic performance of a machine-learning-based coronary CT-FFR (CT-FFR_{ML}) software prototype with a broad range of clinical benefits.[3,4]

However, the potential impact of CT reconstruction algorithms on CT-FFR_{ML} derivation has not been sufficiently investigated and the impact of different algorithms has not been evaluated in the same patient. Therefore, this study sought to assess and compare the influence of iterative reconstruction in image space (IRIS) and filtered back-projection (FBP) reconstruction algorithms on CT-FFR_{ML} values and processing time using machine-learning-based software on a regular workstation.

2. Methods

2.1. Patient population

This retrospective single center study was approved by the local Institutional Review Board with a waiver for informed consent. The study flowchart and enrollment criteria are presented in Fig. 1. Sixty-one consecutive patients who underwent CCTA at our institution between May 2010 and January 2014 were included.

2.2. CT image acquisition protocol and image reconstruction

All CT scans were performed on a 2nd generation dual-source CT system (Somatom Definition Flash; Siemens Healthineers, Forchheim, Germany). CCTA protocol selection was performed as previously described.[3] IRIS series were reconstructed with the "I26f" algorithm ("kernel") and a strength factor of 3, while the "B26f" vascular kernel was used for the FBP series.

2.3. CT-FFR_{ML} analysis and image quality assessment

CT-FFR_{ML} computation was performed using an on-site machine-learning software prototype (cFFR version 3.0, Siemens Healthineers, not commercially available). A 5-point Likert scale was used to rate CCTA image quality according to vessel opacification, structural discontinuity, quality of contour delineation, and general image impression (0 = very poor, 1 = poor, 2 = fair, 3 = good, 4 = excellent). An observer (DM) computed CT-FFR_{ML} values twice for each patient, maintaining a three-week interval between analyses to minimize recall bias. After defining the vessel centerline, lumen, and stenosis, the software allowed for the computation of coronary blood flow and pressures along a patient-specific 3D coronary tree, as previously described.[1,5] CT-FFR_{ML} values were determined for the left main (LM) coronary artery, proximal, middle, and distal segments of the left anterior descending (LAD) and right coronary arteries (RCA), as well as proximal and distal segments of the circumflex artery (CX). Notably, CT-FFR_{ML} measurements were computed distal to lesions with ≥50% luminal stenosis. CT-FFR_{ML} processing time was recorded. Ten patients had invasive FFR correlations available. CT-FFR_{ML} and invasive FFR values ≤ 0.80 defined a flow-limiting stenosis.[6,7]

2.4. Statistical analysis

Pearson's correlation coefficient (r) was used to assess correlations

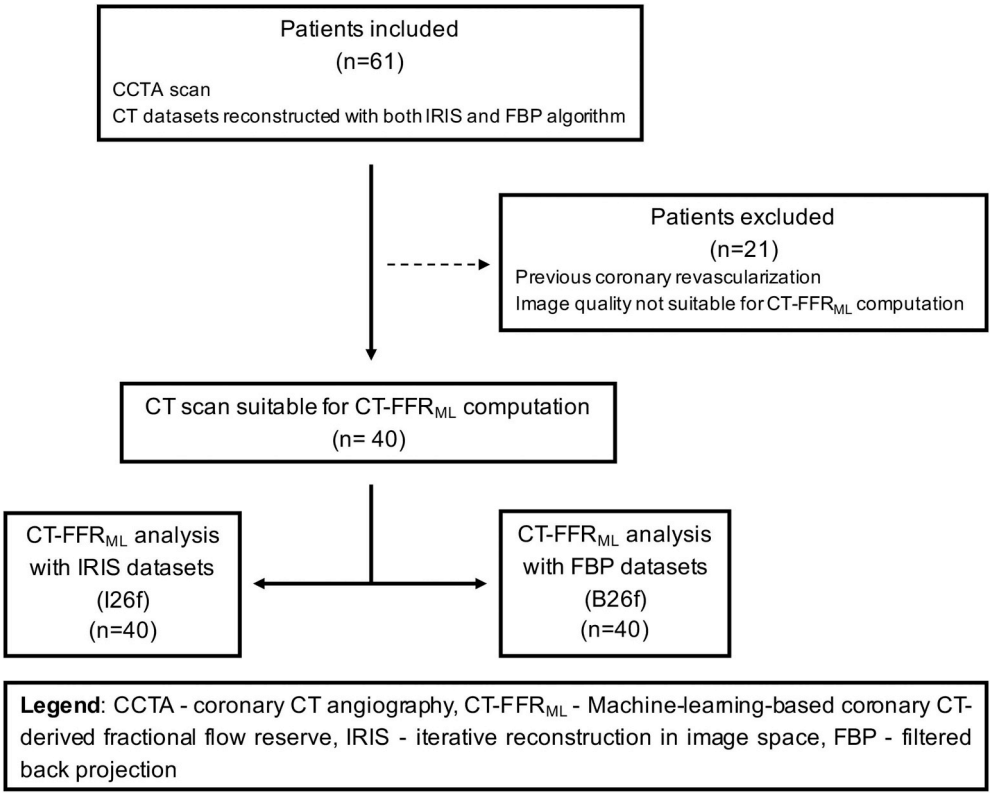

Fig. 1. Study flowchart detailing enrollment, scanning procedures, and CT-FFR_{ML} computation.

Table 1
Baseline population characteristics.

	Total population (n = 40)	Patients with invasive FFR (n = 10)	*p*-value
Patients	40	10	
Male	23 (58%)	5 (50%)	0.816
Age	59 ± 11	65 ± 12	0.792
Weight	79 ± 24	85.4 ± 26.8	0.401
Height	172.7 ± 15.6	166.4 ± 85.4	0.211
BMI	29.2 ± 6.7	30 ± 6	0.426
CV Risk factors			
Hypertension	27 (67%)	8 (80%)	0.234
Diabetes	7 (18%)	2 (20%)	0.316
Dyslipidemia	27 (68%)	8 (80%)	0.234
Smoking history	31 (78%)	8 (80%)	0.687
Family history of CAD	24 (60%)	5 (50%)	0.665

Data are presented as mean ± standard deviation, numbers with percentages (%), or median with interquartile range if not normally distributed.
Legend: CV - cardiovascular; BMI - body mass index; CAD - coronary artery disease; FFR - fractional flow reserve.

between IRIS and FBP-derived CT-FFR$_{ML}$ values; differences were assessed using Wilcoxon testing. Sensitivity, specificity, and diagnostic accuracy were calculated for each reconstruction technique for the detection of significant CAD using invasive catheterization as the reference standard. Diagnostic accuracy was compared using the McNemar test. All statistical analyses were performed using SPSS 24.0 (SPSS Inc., Chicago, Illinois). A *p*-value ≤0.05 was considered statistically significant.

3. Results

3.1. Patient population

Table 1 shows baseline population characteristics. Of the 61 patients, 5 (8%) with coronary revascularization and 16 (26%) with poor image quality were excluded. Therefore, 40 patients were included (23 men (57%), mean age 59 ± 10 years).

3.2. CT-FFR$_{ML}$ results and time of analysis

In total, 160 vessels and 420 segments were analyzed. Image quality of IRIS-reconstructed CCTA datasets were rated significantly higher (2.88 ± 0.83) than FBP datasets (2.53 ± 0.78, $p \leq 0.001$) (Fig. 2).

Table 2
Time requirements, per-vessel, and per-segment CT-FFR$_{ML}$ values for IRIS and FBP CT datasets.

	IRIS	FBP	*p*-value	Pearson's correlation (r)
Time (min)	16 ± 5	20 ± 10	0.021*	
CT-FFR$_{ML}$ values				
Per-segment				
Proximal	0.99 ± 0.03	0.99 ± 0.02	0.008*	0.73
Middle	0.92 ± 0.09	0.93 ± 0.07	0.050*	0.67
Distal	0.80 ± 0.20	0.83 ± 0.15	≤0.001*	0.43
Per-vessel				
LM	1 ± 0.1	1 ± 0.1	0.094	0.74
LAD	0.88 ± 0.18	0.87 ± 0.16	0.002*	0.76
CX	0.93 ± 0.17	0.90 ± 0.16	0.024*	0.53
RCA	0.95 ± 0.12	0.96 ± 0.10	0.002*	0.70

Data are presented as mean ± standard deviation, numbers with percentages (%), or median with interquartile range if not normally distributed; * indicates statistical significance between IRIS and FBP datasets.
Legend: CT-FFR$_{ML}$ Machine-learning-based coronary CT-derived fractional flow reserve; IRIS - iterative reconstruction in image space; FBP - filtered back projection; LM - left main; LAD - left anterior descending; CX - circumflex artery; RCA - right coronary artery.

Per-vessel analysis revealed significantly different CT-FFR$_{ML}$ values between reconstruction techniques for the LAD, RCA, and CX, but not for the LM (Table 2, Fig. 3). Correlation between the two algorithms was high for the LM, LAD, and RCA, whereas CX artery values showed moderate correlation (Table 2, Fig. 3). Per-segment analysis revealed significantly different CT-FFR$_{ML}$ values between the two techniques for proximal, middle, and distal segments (Table 2). Proximal and middle segments showed a high correlation between the two algorithms; however, distal segments demonstrated a weak correlation between techniques (Table 2 and Fig. 3). In patients without invasive FFR, 41/85 (48%) lesions with ≥50% luminal stenosis were identified; however, in 12 of those lesions, the diagnosis for significant ischemia was positive based on the IRIS algorithm, but negative according to the FBP dataset. Invasive FFR measurements were available in 10 patients and a comparison with corresponding CT-FFR$_{ML}$ values revealed no difference in diagnostic accuracy between the two reconstructions (both 81.8%, $p = 1.000$), with identical sensitivities (87.5%) and specificities (66.67%, $p = 1.000$). Per-lesion CT-FFR$_{ML}$ values showed a moderate correlation with invasive FFR for both IRIS (r = 0.53) and FBP (r = 0.49) datasets. CT-FFR$_{ML}$ processing time was significantly shorter

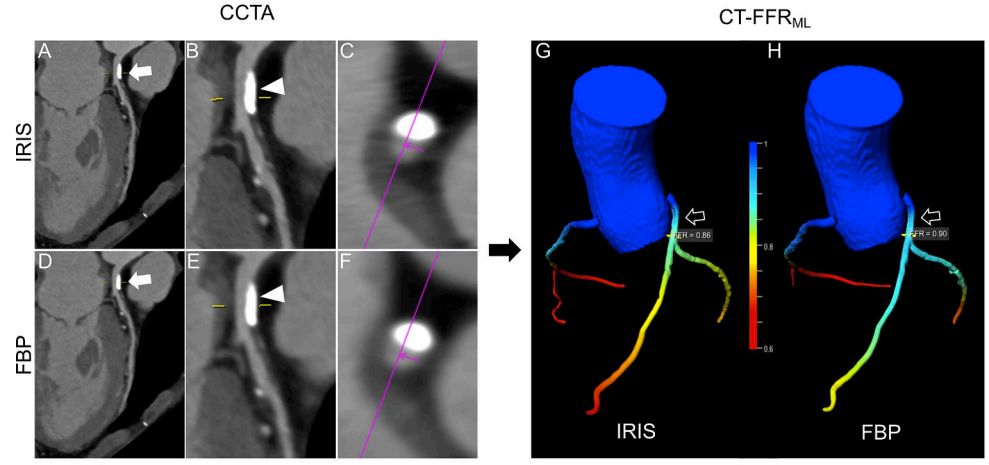

CCTA - coronary computed tomography angiography; IRIS - iterative reconstruction in image space; FBP - filtered back projection; CT-FFR$_{ML}$ - Machine-learning-based coronary CT-derived fractional flow reserve

Fig. 2. Curved MPR (A) and transverse section (C) of IRIS and corresponding FBP datasets (D and F) showing a calcified plaque (A and D, white arrows) causing moderate stenosis of the LM artery in a 49-year old woman. B and E show a close-up of the calcified plaque (white arrowhead). IRIS (G) and FBP-based (H) color-coded 3D mesh reveals different values (CT-FFR$_{ML}$: 0.86 vs 0.90). (For interpretation of the references to color in this figure legend, the reader is referred to the Web version of this article.)

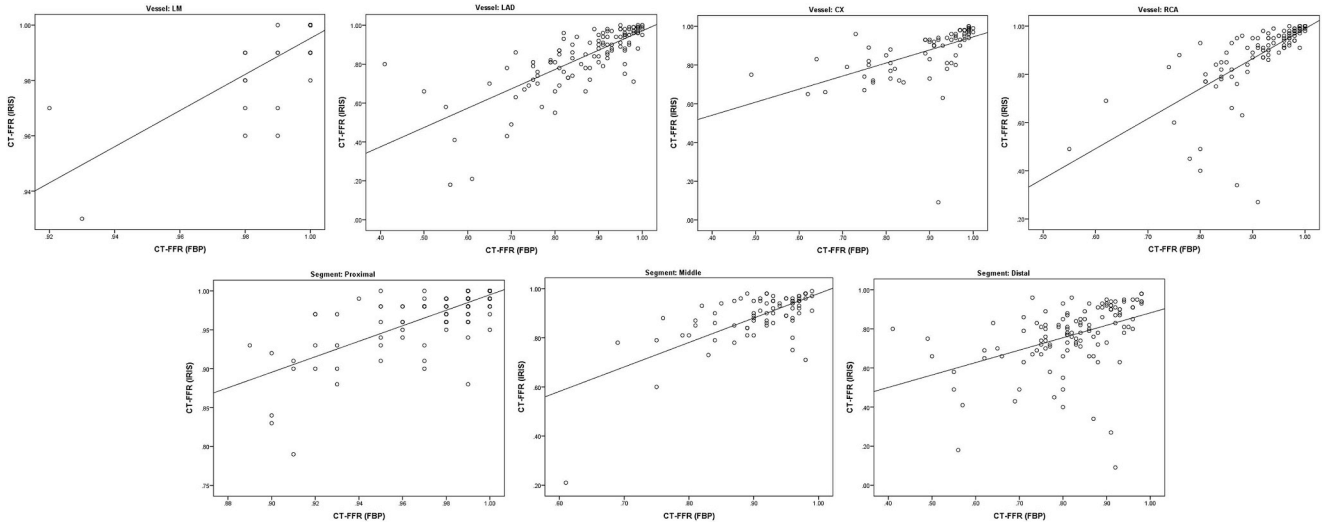

Fig. 3. Scatterplots showing per-vessel (upper) and per-segment (lower) correlation of IRIS- and FBP-based CT-FFR$_{ML}$. Same legend as Table 2.

using IRIS datasets compared to FBP (15.9 vs. 19.8 min, respectively, $p = 0.021$).

4. Discussion

This study investigated the influence of IRIS and FBP on the results and processing time of CT-FFR$_{ML}$. Results demonstrate that IRIS and FBP-reconstructed datasets lead to significantly different CT-FFR$_{ML}$ results, despite maintaining moderate-high correlations. The influence of IR on specific aspects of CCTA has been largely documented (i.e. calcium scoring).[8–10] In prior investigations, differences between reconstruction algorithms were likely attributable to reduced image noise and overall improved image quality.[10,11] Thus, we believe our findings somewhat resemble what was already addressed.

Additionally, in accordance with previous studies, our subgroup analysis performed on patients with invasive FFR (n = 10) showed comparable diagnostic accuracy for detecting lesion-specific ischemia.[1,12] Nonetheless, in patients without invasive FFR, 12 lesions with ≥50% luminal stenosis had a corresponding CT-FFR$_{ML}$ positive for ischemia with IRIS, but non-ischemic with FBP. Interestingly, this discrepancy may lead to varying patient management strategies if CT-FFR was used in a stand-alone clinical fashion.

The significantly faster CT-FFR$_{ML}$ analysis achieved with IRIS-based datasets was another important finding. The timeliness afforded by IRIS can likely be attributed to decreased image noise, which allows for improved automated vessel segmentation and a reduced number of manual coronary segmentation corrections, as previously reported.[13]

Our study should be considered hypothesis-generating, as it highlights a topic that has been largely neglected in the scientific discussion of a novel application. However, our investigation has several limitations beyond its retrospective nature. First, the investigation was performed on a small patient population. Studies with larger cohorts are advisable to confirm or extend our findings. Second, not all technical CT parameters were evaluated, since we only included a strength factor of 3. Prospective studies are warranted to elucidate additional sources of disparity between iterative and FBP datasets, particularly with the new generation of iterative reconstruction algorithms. Lastly, invasive FFR measurements were not available in all patients.

In conclusion, the present study demonstrates that CT reconstruction algorithms influence CT-FFR$_{ML}$ analysis results, thus warranting further investigations to assess clinical implications and develop suitable guidelines. Additionally, iterative reconstruction can improve CT-FFR$_{ML}$ post-processing speed.

Disclosures

Dr. Schoepf receives institutional research support from Astellas, Bayer HealthCare, General Electric Healthcare, and Siemens Healthineers. Drs. De Cecco and Varga-Szemes receive institutional research support from Siemens Healthineers. Dr. De Cecco has received consulting fees from Bayer HealthCare. Dr. Schoepf has received consulting or speaking fees from Bayer, Guerbet, HeartFlow, and Siemens Healthineers. The other authors have no conflict of interest to disclose. Workstation-based flow computations of coronary blood flow are not currently approved by the Food and Drug Administration.

Conflict of interest form

Dr. Schoepf receives institutional research support from Astellas, Bayer HealthCare, General Electric Healthcare, and Siemens Healthineers. Drs. De Cecco and Varga-Szemes receive institutional research support from Siemens Healthineers. Dr. De Cecco has received consulting fees from Bayer Healthcare. Dr. Schoepf has received consulting or speaking fees from Bayer, Guerbet, HeartFlow, and Siemens Healthineers. The other authors have no conflict of interest to disclose. Workstation-based flow computations of coronary blood flow are not currently approved by the Food and Drug Administration.

Appendix A. Supplementary data

Supplementary data to this article can be found online at https://doi.org/10.1016/j.jcct.2018.10.026.

References

1. Tesche C, De Cecco CN, Albrecht MH, et al. Coronary CT angiography–derived fractional flow reserve. *Radiology*. 2017. https://doi.org/10.1148/radiol.2017162641.
2. Nørgaard BL, Leipsic J, Gaur S, et al. Diagnostic performance of noninvasive fractional flow reserve derived from coronary computed tomography angiography in suspected coronary artery disease: the NXT trial (Analysis of Coronary Blood Flow Using CT Angiography: next Steps). *J Am Coll Cardiol*. 2014. https://doi.org/10.1016/j.jacc.2013.11.043.
3. Tesche C, Cecco CN De, Baumann S, et al. Coronary CT angiography–derived fractional flow reserve: machine learning algorithm versus computational fluid dynamics modeling. Radiology. 0(0):171291. doi: https://doi.org/10.1148/radiol.2018171291.
4. Yang DH, Kim YH, Roh JH, et al. Diagnostic performance of on-site CT-derived fractional flow reserve versus CT perfusion. *Eur Heart J Cardiovasc Imaging*. 2017. https://doi.org/10.1093/ehjci/jew094.
5. Tesche C, De Cecco CN, Caruso D, et al. Coronary CT angiography derived

morphological and functional quantitative plaque markers correlated with invasive fractional flow reserve for detecting hemodynamically significant stenosis. *J Cardiovasc Comput Tomogr*. 2016. https://doi.org/10.1016/j.jcct.2016.03.002.
6. Bech GJW, De Bruyne B, Pijls NHJ, et al. Fractional flow reserve to determine the appropriateness of angioplasty in moderate coronary stenosis: a randomized trial. *Circulation*. 2001. https://doi.org/10.1161/01.CIR.103.24.2928.
7. Coenen A, Lubbers MM, Kurata A, et al. Fractional flow reserve computed from noninvasive CT angiography data: diagnostic performance of an on-site clinician-operated computational fluid dynamics algorithm. *Radiology*. 2015. https://doi.org/10.1148/radiol.14140992.
8. Renker M, Nance JW, Schoepf UJ, et al. Evaluation of heavily calcified vessels with coronary CT angiography: comparison of iterative and filtered back projection image reconstruction. *Radiology*. 2011. https://doi.org/10.1148/radiol.11103574.
9. Wang R, Schoepf UJ, Wu R, et al. Diagnostic accuracy of coronary ct angiography: comparison of filtered back projection and iterative reconstruction with different strengths. *J Comput Assist Tomogr*. 2014. https://doi.org/10.1097/RCT.0000000000000005.
10. Geyer LL, Glenn GR, De Cecco CN, et al. CT evaluation of small-diameter coronary artery stents: effect of an integrated circuit detector with iterative reconstruction. *Radiology*. 2015. https://doi.org/10.1148/radiol.15140427.
11. Kurata A, Dharampal A, Dedic A, et al. Impact of iterative reconstruction on CT coronary calcium quantification. *Eur Radiol*. 2013. https://doi.org/10.1007/s00330-013-3022-8.
12. Renker M, Schoepf UJ, Wang R, et al. Comparison of diagnostic value of a novel noninvasive coronary computed tomography angiography method versus standard coronary angiography for assessing fractional flow reserve. *Am J Cardiol*. 2014. https://doi.org/10.1016/j.amjcard.2014.07.064.
13. Spears JR, Schoepf UJ, Henzler T, et al. Comparison of the effect of iterative reconstruction versus filtered back projection on cardiac CT postprocessing. *Acad Radiol*. 2014. https://doi.org/10.1016/j.acra.2013.11.008.